Discretization of the Boltzmann equation in velocity space using a Galerkin approach

Jonas Tölke, Manfred Krafczyk, Manuel Schulz, Ernst Rank *

Lehrstuhl für Bauinformatik, Technische Universität München, 80290 München, Germany

Abstract

A method for the discretization of the Boltzmann equation in velocity space via a Galerkin procedure with Hermite polynomials as trial and test functions is proposed. This procedure results in a set of partial differential equations, which is an alternative to the lattice-Boltzmann equations. These PDEs are discretized using an explicit finite difference scheme and a numerical example shows the validity of the approach. © 2000 Elsevier Science B.V. All rights reserved.

Keywords: Lattice-Boltzmann; Kinetic theory

1. Introduction

The BGK approximation [9] of the Boltzmann equation

$$\frac{\partial f}{\partial t} + \vec{\xi} \cdot \frac{\partial f}{\partial \vec{x}} = -\frac{1}{\tau}\big(f - f^{\text{eq}}(\rho, \vec{u})\big), \tag{1}$$

is a mathematical model for the motion of a fluid at the microscopic level. Here $f(t, \vec{\xi}, \vec{x})$ is the particle distribution function, $\vec{\xi}$ the microscopic velocity and τ the relaxation time. It is more general than the Navier–Stokes equations but it has also more independent variables. The macroscopic flow properties like density ρ, momentum $\rho\vec{u}$ and the pressure tensor $P_{\alpha\beta}$ are given by the following relations [3]:

$$\rho = \int_{-\infty}^{\infty} f \, \mathrm{d}\vec{\xi}, \tag{2}$$

$$\rho u_\alpha = \int_{-\infty}^{\infty} \xi_\alpha f \, \mathrm{d}\vec{\xi}, \tag{3}$$

$$P_{\alpha\beta} = \int_{-\infty}^{\infty} (\xi_\alpha - u_\alpha)(\xi_\beta - u_\beta) f \, \mathrm{d}\vec{\xi}. \tag{4}$$

---

* Corresponding author. E-mail: rank@server.inf.bauwesen.tu-muenchen.de.

The pressure tensor is related to the stresses $\sigma_{\alpha\beta}$ by

$$P_{\alpha\beta} = \mathbf{I}p - \sigma_{\alpha\beta}, \tag{5}$$

where $p = \frac{1}{3}\operatorname{tr}\{P_{\alpha\beta}\} = RT\rho$ is the scalar pressure. The solution for a fluid in uniform state is given by the local equilibrium distribution function:

$$f^{\mathrm{eq}} = \frac{\rho}{(2\pi RT)^{D/2}} \exp\left(-\frac{(\vec{\xi} - \vec{u})^2}{2RT}\right), \tag{6}$$

where R is the gas-constant, T is the temperature and D the dimension of space. The absolute equilibrium distribution function is given by setting $\vec{u} = 0$ in equation (6). It has been shown that the continuous lattice-Boltzmann equation

$$\frac{\partial f_i}{\partial t} + \vec{\xi}_{i\alpha}\frac{\partial f_i}{\partial x_\alpha} = -\frac{1}{\tau}\left(f_i - \tilde{f}_i^{\mathrm{eq}}(\rho, \vec{u})\right) \tag{7}$$

can be derived from a numerical integration of the Boltzmann Eq. (1) in velocity space [1]. Discretization of Eq. (7) in space and time with finite difference formulas yields the (discrete) lattice-Boltzmann equation

$$f_i(t + \triangle t, \vec{x} + \vec{\xi}_i \triangle t) - f_i(t, \vec{x}) = -\frac{1}{\tau}\left(f_i(t, \vec{x}) - \tilde{f}_i^{\mathrm{eq}}(t, \vec{x})\right), \tag{8}$$

which has been widely used as a computational tool for the simulation of fluid flow. An alternative way, proposed here, is to use a Galerkin procedure with *analytical* integration of the Boltzmann equation (1) in velocity space for obtaining a low order approximation of the Boltzmann equation in velocity space.

2. Hermite polynomials

Hermite polynomials are orthogonal polynomials in the interval $[-\infty, \infty]$ with respect to the weight function $w = \exp(-\frac{x^2}{2})$ [7]:

$$\int_{-\infty}^{\infty} \exp\left(-\frac{x^2}{2}\right) H_i(x) H_j(x) \, \mathrm{d}x = \delta_{ij}\sqrt{2\pi}, \tag{9}$$

where

$$H_1(x) = 1, \quad H_2(x) = x, \quad H_3(x) = \frac{x^2 - 1}{\sqrt{2}}, \quad H_4(x) = \cdots. \tag{10}$$

Hermite polynomials have the following property:

$$\int_{-\infty}^{\infty} x^n H_i(x) \, \mathrm{d}x = 0 \quad \text{if } i > n + 1. \tag{11}$$

3. Ansatz function

The mass and the momentum equation are given by the velocity moments $\psi_0 = 1$ and $\psi_1 = \vec{\xi}$ of the Boltzmann equation (1)

$$\frac{\partial}{\partial t} \int \psi_i f \, \mathrm{d}\vec{\xi} + \nabla \cdot \int \psi_i \vec{\xi} f \, \mathrm{d}\vec{\xi} = 0, \quad i \in \{0, 1\}. \tag{12}$$

The moments of the collision operator vanish because the ψ_i are collisional invariants [9]. Expanding the distribution function in Hermite polynomials and exploiting property (11), the mass equation is determined by Hermite coefficients up to first and the momentum equation up to second order. Therefore we use the following *ansatz* with trial functions of at most second order, restricting the analysis to a 2D problem for simplicity.

$$
\hat{f} = \frac{1}{2\pi RT} \exp\left(-\frac{\xi_1{}^2 + \xi_2{}^2}{2RT}\right) \sum_{k=1}^{6} a_k(t, x_1, x_2) \varphi_k(\xi_1, \xi_2),
\tag{13}
$$

where $a_k(t, x_1, x_2)$ are the coefficients of the expansion and $\varphi_k(\xi_1, \xi_2)$ the following trial functions:

$$
\varphi_1 = H_1\left(\frac{\xi_1}{\sqrt{RT}}\right) H_1\left(\frac{\xi_2}{\sqrt{RT}}\right) = 1,
\tag{14}
$$

$$
\varphi_2 = H_2\left(\frac{\xi_1}{\sqrt{RT}}\right) H_1\left(\frac{\xi_2}{\sqrt{RT}}\right) = \frac{\xi_1}{\sqrt{RT}},
\tag{15}
$$

$$
\varphi_3 = H_1\left(\frac{\xi_1}{\sqrt{RT}}\right) H_2\left(\frac{\xi_2}{\sqrt{RT}}\right) = \frac{\xi_2}{\sqrt{RT}},
\tag{16}
$$

$$
\varphi_4 = H_2\left(\frac{\xi_1}{\sqrt{RT}}\right) H_2\left(\frac{\xi_2}{\sqrt{RT}}\right) = \frac{\xi_1 \xi_2}{RT},
\tag{17}
$$

$$
\varphi_5 = H_3\left(\frac{\xi_1}{\sqrt{RT}}\right) H_1\left(\frac{\xi_2}{\sqrt{RT}}\right) = \frac{1}{\sqrt{2}}\left(\frac{\xi_1{}^2}{RT} - 1\right),
\tag{18}
$$

$$
\varphi_6 = H_1\left(\frac{\xi_1}{\sqrt{RT}}\right) H_3\left(\frac{\xi_2}{\sqrt{RT}}\right) = \frac{1}{\sqrt{2}}\left(\frac{\xi_2{}^2}{RT} - 1\right).
\tag{19}
$$

Ansatz (13) is similar to the one suggested by Grad for the '13-moment-system' [3], yet having the following differences:

- As we are interested in nearly incompressible and isothermal flows, we ignore the energy equation and use only a second order approximation (Grad used a third order approximation).
- In nearly incompressible flows the macroscopic velocity is much smaller than the average velocity of the particles. Therefore we expand *ansatz* (13) about the *absolute* equilibrium (Grad expanded about the *local* equilibrium).

The macroscopic variables in terms of the Hermite coefficients are given by

$$
\rho = \iint\limits_{-\infty}^{\infty} \hat{f}\, d\xi_1 d\xi_2 = a_1,
\tag{20}
$$

$$
u_1 = \iint\limits_{-\infty}^{\infty} \xi_1 \hat{f}\, d\xi_1 d\xi_2 = \frac{a_2 \sqrt{RT}}{a_1},
\tag{21}
$$

$$
u_2 = \iint\limits_{-\infty}^{\infty} \xi_2 \hat{f}\, d\xi_1 d\xi_2 = \frac{a_3 \sqrt{RT}}{a_1},
\tag{22}
$$

$$
\sigma_{11} = -\iint\limits_{-\infty}^{\infty} (\xi_1 - u_1)^2 \hat{f}\, d\xi_1 d\xi_2 + RT\rho = -RT\left(\sqrt{2} a_5 - \frac{a_2^2}{a_1}\right),
\tag{23}
$$

$$
\sigma_{22} = -\iint\limits_{-\infty}^{\infty} (\xi_2 - u_2)^2 \hat{f}\, d\xi_1 d\xi_2 + RT\rho = -RT\left(\sqrt{2} a_6 - \frac{a_3^2}{a_1}\right),
\tag{24}
$$

$$\sigma_{12} = -\iint\limits_{-\infty}^{\infty} (\xi_1 - u_1)(\xi_2 - u_2)\hat{f}\,\mathrm{d}\xi_1\mathrm{d}\xi_2 = -RT\left(a_4 - \frac{a_2 a_3}{a_1}\right). \tag{25}$$

In contrast to the standard LBGK scheme an inverse relationship can easily be identified:

$$a_1 = \rho, \tag{26}$$

$$a_2 = \frac{u_1 \rho}{\sqrt{RT}}, \tag{27}$$

$$a_3 = \frac{u_2 \rho}{\sqrt{RT}}, \tag{28}$$

$$a_4 = \frac{u_1 u_2 \rho - \sigma_{12}}{RT}, \tag{29}$$

$$a_5 = \frac{\sqrt{2}}{2}\frac{u_1{}^2\rho - \sigma_{11}}{RT}, \tag{30}$$

$$a_6 = \frac{\sqrt{2}}{2}\frac{u_2{}^2\rho - \sigma_{22}}{RT}. \tag{31}$$

Thus one can compute the Hermite coefficients from the macroscopic quantities and vice versa in a *unique* way.

4. Galerkin procedure

Inserting *ansatz* (13) in the Boltzmann equation implies a residual depending on the unknown Hermite coefficients:

$$R(a_1,\ldots,a_6,\xi_1,\xi_2) = \frac{\partial \hat{f}}{\partial t} + \vec{\xi}\frac{\partial \hat{f}}{\partial \vec{x}} + \frac{\hat{f} - f^{\mathrm{eq}}(a_1, a_2, a_3)}{\tau}. \tag{32}$$

To approximate the exact solution of the Boltzmann equation, two approaches can be used:

(a) Collocation procedure:
The residual is set to zero at certain quadrature points. Following [1], conservation laws can be forced to hold exactly if a modified collision operator $-\frac{1}{\tau}(\hat{f} - \tilde{f}^{\mathrm{eq}})$ is used, where $\tilde{f}^{\mathrm{eq}}$ is an expansion of f^{eq} using the 6 Hermite polynomials (14)–(19). This procedure results in the continuous lattice-Boltzmann equation (7).

(b) Galerkin procedure:
The residual is minimized in an integral sense, where the trial functions are also used as test functions:

$$\iint\limits_{-\infty}^{\infty} \varphi_k\, R\mathrm{d}\xi_1\mathrm{d}\xi_2 = 0, \quad k = 1,\ldots,6. \tag{33}$$

Using the second approach and explicitly calculating the integrals one obtains the following set of partial differential equations:

$$\frac{\partial a_1}{\partial t} + \sqrt{RT}\left(\frac{\partial a_2}{\partial x_1} + \frac{\partial a_3}{\partial x_2}\right) = 0, \tag{34}$$

$$\frac{\partial a_2}{\partial t} + \sqrt{RT}\left(\frac{\partial a_1}{\partial x_1} + \sqrt{2}\frac{\partial a_5}{\partial x_1} + \frac{\partial a_4}{\partial x_2}\right) = 0, \tag{35}$$

$$\frac{\partial a_3}{\partial t} + \sqrt{RT}\left(\frac{\partial a_4}{\partial x_1} + \frac{\partial a_1}{\partial x_2} + \sqrt{2}\frac{\partial a_6}{\partial x_2}\right) = 0, \tag{36}$$

$$\frac{\partial a_4}{\partial t} + \sqrt{RT}\left(\frac{\partial a_3}{\partial x_1} + \frac{\partial a_2}{\partial x_2}\right) = -\frac{1}{\tau}\left(a_4 - \frac{a_2 a_3}{a_1}\right), \tag{37}$$

$$\frac{\partial a_5}{\partial t} + \sqrt{2RT}\frac{\partial a_2}{\partial x_1} = -\frac{1}{\tau}\left(a_5 - \frac{a_2{}^2}{\sqrt{2}a_1}\right), \tag{38}$$

$$\frac{\partial a_6}{\partial t} + \sqrt{2RT}\frac{\partial a_3}{\partial x_2} = -\frac{1}{\tau}\left(a_6 - \frac{a_3{}^2}{\sqrt{2}a_1}\right). \tag{39}$$

Note, that the spatial differential operator of these equations is linear, but not diagonal as in the lattice-Boltzmann equations (7). Eqs. (34)–(39) can now be solved numerically using appropriate schemes.

5. Recovering the Navier–Stokes equations

Following the basic idea of Grad [3], the Navier–Stokes equations can be recovered without using the Chapman–Enskog expansion from system (34)–(39), under the condition that the relaxation time (or the mean free path) and the Mach number goes to zero. We have three time scales τ, T_0 and T_1 with the relation $\tau \ll T_0 \ll T_1$. T_1 is the macroscopic time scale where changes in the density and momentum occur. T_0 is an intermediate time scale small enough to consider the values of the macroscopic quantities density and momentum to be independent of time. Time scale τ is of the order of the collision time. Consider now an equation with an arbitrary function $g(t)$ and a small parameter τ on the time interval $[0, T_0]$:

$$\frac{\partial g(t)}{\partial t} + \frac{g(t)}{\tau} + C = 0, \quad t \in [0, T_0], \tag{40}$$

where C is a constant. The solution is

$$g(t) = -\tau C + C_1 \exp\left(-\frac{t}{\tau}\right), \tag{41}$$

where C_1 is a constant. The function $g(t)$ approaches steady state exponentially with time scale τ. If in Eqs. (37)–(39) the parameter τ becomes very small the functions a_1, a_2 and a_3 (density and momentum) can be considered to be independent of time on the scale T_0. Thus a_4, a_5 and a_6 are of type $g(t)$ in Eq. (40). After a few collision times a quasi equilibrium sets up and the coefficients a_4, a_5, a_6 in terms of macroscopic variables can be expressed on a macroscopic time scale as

$$a_4 = -\tau\left(\frac{\partial \rho u_2}{\partial x_1} + \frac{\partial \rho u_1}{\partial x_2}\right) + \frac{u_1 u_2 \rho}{RT}, \tag{42}$$

$$a_5 = -\tau\sqrt{2}\frac{\partial \rho u_1}{\partial x_1} + \frac{u_1{}^2 \rho}{\sqrt{2}RT}, \tag{43}$$

$$a_6 = -\tau\sqrt{2}\frac{\partial \rho u_2}{\partial x_2} + \frac{u_2{}^2 \rho}{\sqrt{2}RT}. \tag{44}$$

Substituting the coefficients a_i using (26)–(28) and (42)–(44) in Eqs. (34)–(36) one obtains:

$$\frac{\partial \rho}{\partial t} + \frac{\partial \rho u_1}{\partial x_1} + \frac{\partial \rho u_2}{\partial x_2} = 0, \tag{45}$$

$$\frac{\partial \rho u_1}{\partial t} + \frac{\partial \rho u_1{}^2}{\partial x_1} + \frac{\partial \rho u_1 u_2}{\partial x_2} + RT\frac{\partial \rho}{\partial x_1} = \frac{\partial \sigma_{11}}{\partial x_1} + \frac{\partial \sigma_{12}}{\partial x_2}, \tag{46}$$

$$\frac{\partial \rho u_2}{\partial t} + \frac{\partial \rho u_1 u_2}{\partial x_1} + \frac{\partial \rho u_2{}^2}{\partial x_2} + RT\frac{\partial \rho}{\partial x_2} = \frac{\partial \sigma_{12}}{\partial x_1} + \frac{\partial \sigma_{22}}{\partial x_2}, \tag{47}$$

$$\sigma_{\alpha\beta} = RT\tau\left(\frac{\partial \rho u_\alpha}{\partial x_\beta} + \frac{\partial \rho u_\beta}{\partial x_\alpha}\right). \tag{48}$$

Assuming low Mach-number and therefore nearly incompressible flow, this gives the correct relation between the stresses and the flow field with a kinematic viscosity $\nu = RT\tau$. Also the equation of state is given by $p = RT\rho$. From the above considerations it can be seen, that for *stationary* problems the magnitude of τ is irrelevant for recovering the correct macroscopic equations, whereas for *transient* problems it has to be small compared to a typical macroscopic time scale.

6. Numerical discretization in the time-space domain

System (34)–(39) can be written in the from

$$\frac{\partial}{\partial t}\vec{a} + \mathbf{A}\frac{\partial}{\partial x_1}\vec{a} + \mathbf{B}\frac{\partial}{\partial x_2}\vec{a} = \vec{C}(\vec{a}), \tag{49}$$

where $\vec{a}$ are the Hermite coefficients, $\mathbf{A}$ and $\mathbf{B}$ the matrices of the spatial differential operators and $\vec{C}$ the nonlinear source term. System (49) is discretized using a second order upwind scheme in space on a uniform mesh and a first order explicit Euler scheme in time. Following [2], the matrices $\mathbf{A}$ and $\mathbf{B}$ are split into matrices $\mathbf{A}^+, \mathbf{A}^-$ and $\mathbf{B}^+, \mathbf{B}^-$, corresponding to their eigenvalues $\sqrt{RT}, -\sqrt{RT}, \sqrt{3RT}, -\sqrt{3RT}, 0, 0$ for both matrices.

$$\mathbf{A}^+ = \mathbf{R}\Lambda^+\mathbf{L}, \qquad \mathbf{A}^- = \mathbf{R}\Lambda^-\mathbf{L}. \tag{50}$$

$\mathbf{R}$ is the matrix composed of the right eigenvectors (each column represents an eigenvector) of $\mathbf{A}$, $\mathbf{L}$ is the inverse of $\mathbf{R}$ and $\Lambda^{+/-} = \mathrm{diag}\{\lambda_1^{+/-}, \ldots, \lambda_6^{+/-}\}$ are diagonal matrices composed of the positive and nonpositive eigenvalues. Matrix $\mathbf{B}$ is decomposed in an equivalent manner. The result is

$$\mathbf{A}^+ = \sqrt{RT}\begin{pmatrix} \frac{\sqrt{3}}{6} & \frac{1}{2} & 0 & 0 & \frac{\sqrt{6}}{6} & 0 \\ \frac{1}{2} & \frac{\sqrt{3}}{2} & 0 & 0 & \frac{\sqrt{2}}{2} & 0 \\ 0 & 0 & \frac{1}{2} & \frac{1}{2} & 0 & 0 \\ 0 & 0 & \frac{1}{2} & \frac{1}{2} & 0 & 0 \\ \frac{\sqrt{6}}{6} & \frac{\sqrt{2}}{2} & 0 & 0 & \frac{\sqrt{3}}{3} & 0 \\ 0 & 0 & 0 & 0 & 0 & 0 \end{pmatrix}, \qquad \mathbf{A}^- = \sqrt{RT}\begin{pmatrix} -\frac{\sqrt{3}}{6} & \frac{1}{2} & 0 & 0 & -\frac{\sqrt{6}}{6} & 0 \\ \frac{1}{2} & -\frac{\sqrt{3}}{2} & 0 & 0 & \frac{\sqrt{2}}{2} & 0 \\ 0 & 0 & -\frac{1}{2} & \frac{1}{2} & 0 & 0 \\ 0 & 0 & \frac{1}{2} & -\frac{1}{2} & 0 & 0 \\ -\frac{\sqrt{6}}{6} & \frac{\sqrt{2}}{2} & 0 & 0 & -\frac{\sqrt{3}}{3} & 0 \\ 0 & 0 & 0 & 0 & 0 & 0 \end{pmatrix},$$

$$\mathbf{B}^+ = \sqrt{RT}\begin{pmatrix} \frac{\sqrt{3}}{6} & 0 & \frac{1}{2} & 0 & 0 & \frac{\sqrt{6}}{6} \\ 0 & \frac{1}{2} & 0 & \frac{1}{2} & 0 & 0 \\ \frac{1}{2} & 0 & \frac{\sqrt{3}}{2} & 0 & 0 & \frac{\sqrt{2}}{2} \\ 0 & \frac{1}{2} & 0 & \frac{1}{2} & 0 & 0 \\ 0 & 0 & 0 & 0 & 0 & 0 \\ \frac{\sqrt{6}}{6} & 0 & \frac{\sqrt{2}}{2} & 0 & 0 & \frac{\sqrt{3}}{3} \end{pmatrix}, \qquad \mathbf{B}^- = \sqrt{RT}\begin{pmatrix} -\frac{\sqrt{3}}{6} & 0 & \frac{1}{2} & 0 & 0 & -\frac{\sqrt{6}}{6} \\ 0 & -\frac{1}{2} & 0 & \frac{1}{2} & 0 & 0 \\ \frac{1}{2} & 0 & -\frac{\sqrt{3}}{2} & 0 & 0 & \frac{\sqrt{2}}{2} \\ 0 & \frac{1}{2} & 0 & -\frac{1}{2} & 0 & 0 \\ 0 & 0 & 0 & 0 & 0 & 0 \\ -\frac{\sqrt{6}}{6} & 0 & \frac{\sqrt{2}}{2} & 0 & 0 & -\frac{\sqrt{3}}{3} \end{pmatrix}.$$

Now the following numerical scheme can be defined [2]:

$$\vec{a}_{i,j}^{n+1} = \vec{a}_{i,j}^n - \frac{\Delta t}{2\Delta x}\Big(\mathbf{A}^+\big(3\vec{a}_{i,j}^n - 4\vec{a}_{i-1,j}^n + \vec{a}_{i-2,j}^n\big) + \mathbf{A}^-\big(-\vec{a}_{i+2,j}^n + 4\vec{a}_{i+1,j}^n - 3\vec{a}_{i,j}^n\big)$$

$$+ \mathbf{B}^+\big(3\vec{a}_{i,j}^n - 4\vec{a}_{i,j-1}^n + \vec{a}_{i,j-2}^n\big) + \mathbf{B}^-\big(-\vec{a}_{i,j+2}^n + 4\vec{a}_{i,j+1}^n - 3\vec{a}_{i,j}^n\big)\Big) + \vec{C}(\vec{a}_{i,j}),$$

where n denotes the time step, Δt the time resolution and Δx the mesh resolution. The maximum time step is restricted for reasons of stability. In the case $\tau \ll \Delta x$, the time is restricted by $\Delta t < 2\tau$ (in accordance with [4]).
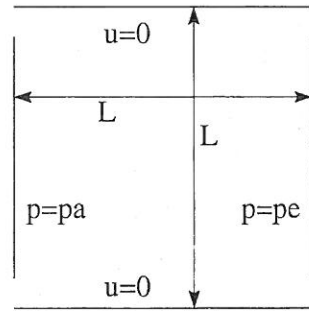
$$pa = 1.0004 \; Pa$$
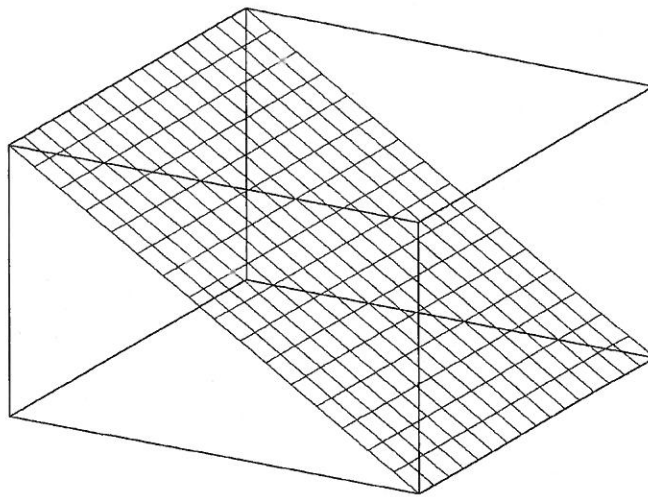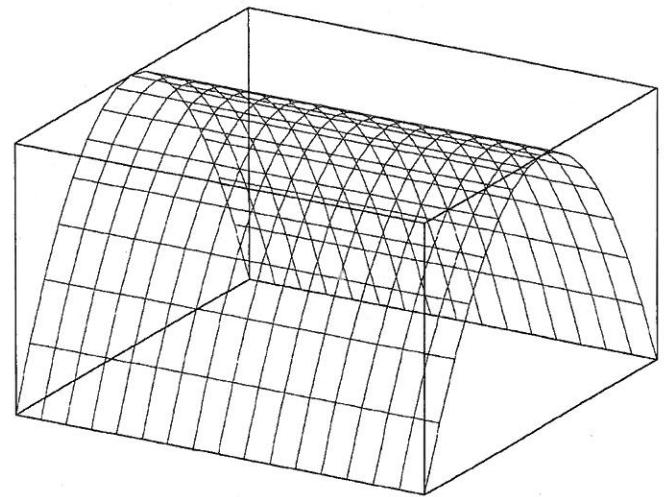$$pe = 0.9996 \; Pa$$
$$RT = 1.0 \; m^2/s^2$$
$$\nu = 0.01 \; m^2/s$$
$$L = 1.0 \; m$$

Fig. 1. Boundary conditions for Poiseuille flow.

(a)   (b)

Fig. 2. Resulting pressure and velocity for Poiseuille flow (65×65 grid).

7. Boundary conditions

Macroscopic boundary conditions can be incorporated into the scheme using relations (20)–(25) and (26)–(31): All Hermite coefficients at the boundary are obtained by linear extrapolation in space from neighboring grid points at each time step [2]. Relations (20)–(25) are then used to obtain the (extrapolated) macroscopic quantities at the boundaries. Now all *known* macroscopic quantities are simply set to their prescribed boundary values. The inverse transformation (26)–(31) gives then the boundary conditions for the next time step. It is possible to incorporate boundary conditions in ρ, u_α and $\sigma_{\alpha\beta}$.

8. Example: Poiseuille flow

In first numerical investigations [10] it was shown, that for arbitrary uniform grids the analytical solution of Couette flow could be reproduced within machine accuracy. Here we will consider the more interesting problem of Poiseuille flow driven by a true pressure difference. The boundary conditions are sketched in Fig. 1 and the parameters are chosen as pointed out in Fig. 1. The maximum velocity of the analytical solution is $u_{\max} = 0.01$ m/s. The velocity profiles for meshes of 9×9, 17×17, 33×33 and 65×65 nodes are shown in Fig. 3(a). The results indicate that a higher order numerical viscosity is introduced by the present numerical scheme, but the convergence rate (see Fig. 3(b), log-scale of the relative error in $u_{\max}$) is quadratic. No edge or inflow/outflow effects are
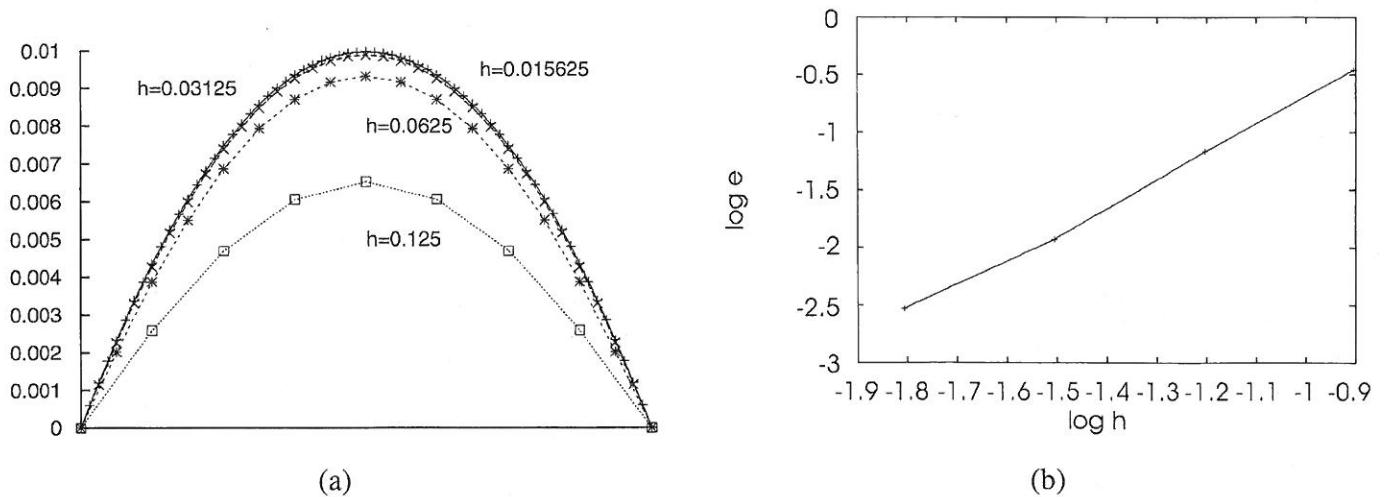
Fig. 3. Results for Poiseuille flow driven by a pressure difference.

observed (Fig. 2). The total error is composed of the discretization and the compressibility error. It should be noted that the compressibility error is much smaller than the discretization error for this example.

9. Discussion and outlook

The system (34)–(39) offers some advantages over the conventional LB equations. It can be discretized using any numerical scheme and offers the following possibilities:

- Decoupling of space and time-resolution: The conventional LB scheme is restricted to a certain value of the parameter τ (and therefore a certain Reynolds-number) due to stability issues. Higher Reynolds-numbers can only be achieved by increasing the size of the computational domain. This implies a penalty of at least $O(n^2)/O(n^3)$ for 2D/3D problems. In the present scheme one has the possibility to decrease the time step to achieve stability.
- The freedom in the choice of the numerical method gives the possibility to use implicit schemes and unstructured meshes.
- There is a unique relationship between the macroscopic variables and the Hermite coefficients, so that boundary conditions are easily implemented. Furthermore a proper implementation of boundary conditions does not decrease the spatial convergence rate as for example the bounce back procedure in the LBGK scheme.

The extension of the Galerkin procedure outlined in this paper to three-dimensional problems is technically straightforward. The *ansatz* requires then 10 trial functions, the Hermite coefficients are related to the 10 independent macroscopic variables density, momentum and the 6 independent components of the stress tensor. The present analysis can also be used to discretize more complex equations than (1) describing multiphase flow as discussed in [5,6]. First results are very promising and will be subject to future publications.

References

[1] X. Shan, X. He, Discretization of the velocity space in solution of the Boltzmann equation, http://xyz.lanl.gov (1997).
[2] C. Hirsch, Num. Comp. of External and Internal Flows (Wiley & Sons, New York, 1989).
[3] H. Grad, On the kinetic theory of rarefied gases, Commun. Pure Appl. Math. 2 (1949) 331–407.
[4] R. Mei, W. Shyy, On the finite difference based lattice-Boltzmann model in curvilinear coordinates, Preprint (1998).
[5] Li-Shi Lou, Unified theory of lattice-Boltzmann models for nonideal gases, Phys. Rev. Lett. 81 (8) (1998) 1618–1621.
[6] X. He, X. Shan, G.D. Doolen, Discrete Boltzmann equation model for nonideal gases, Phys. Rev. E 57 (1) (1998).

[7] J.P. Boyd, Chebyshev and Fourier Spectral Methods (Springer, Berlin, 1989)

[8] Y.H. Quian, D. d'Humieres, P. Lallemand, Lattice BGK models for Navier–Stokes equations, Europhys. Lett. 17 (6) (1992) 479–484.

[9] S. Chapman, T.G. Cowling, The Mathematical Theory of Non-Uniform Gases (Cambridge University Press, 3rd edn., 1990).

[10] J. Tölke, Internal Report, Lehrstuhl für Bauinformatik, Technische Universität München.